Journal of Saudi Chemical Society (2015) **19**, 471–478

King Saud University

Journal of Saudi Chemical Society

www.ksu.edu.sa
www.sciencedirect.com

ORIGINAL ARTICLE

Visible light photocatalytic degradation of 4-chlorophenol using C/ZnO/CdS nanocomposite

Atul B. Lavand, Yuvraj S. Malghe *

Department of Chemistry, The Institute of Science, Mumbai 400032, Maharashtra, India

Received 2 March 2015; revised 28 June 2015; accepted 2 July 2015
Available online 10 July 2015

KEYWORDS

Visible light;
Photocatalysis;
C doped ZnO;
CdS;
Nanocomposite

Abstract C/ZnO/CdS nanocomposite was synthesized using the microemulsion method. Nanocomposite synthesized in the present work was characterized using X-ray diffractometer (XRD), scanning electron microscope (SEM), energy dispersive X-ray spectroscopy (EDX) transmission electron microscope (TEM), diffuse reflectance and photoluminescence (PL) spectroscopy. TEM study shows that CdS nanoparticles are successfully anchored on the surface of C doped ZnO nanorods. UV–visible spectrum of C/ZnO/CdS nanocomposite shows a red shift. CdS nanoparticles work as photo sensitizers to expand the photo-response of C doped ZnO to the visible region. Photoluminescence (PL) spectroscopy reveals evidence for interaction between C/ZnO and CdS. PL quenching observed for C/ZnO/CdS nanocomposite is attributed to improved charge separation properties, which increases its photocatalytic efficiency. C/ZnO/CdS nanocomposite exhibits exceptionally high photocatalytic activity for degradation of 4-chlorophenol (CP) via Z-scheme mechanism. C/ZnO/CdS nanocomposite is a highly stable and reusable photocatalyst.

1. Introduction

Phenolic compounds are toxic, hazardous, and common pollutants in industrial waste water that originates from coal conversion and petroleum refining industries [1,2]. Chlorophenols (CPs) are used as herbicides, pesticides and wood preservatives. Among the CPs, 4-chlorophenol (4-CP) is used in the production of dyes, pesticides and drugs. CP's are most vulnerable water pollutants, which cause serious damage to the vital organs of human beings. Hence the removal of CP from the waste water is very essential. Heterogeneous semiconductor photocatalysis is a promising solution/alternative for the degradation of organic pollutants from water [3–6]. Photocatalysis is based on the principle that when a semiconductor is exposed to a light source with appropriate wavelength, the electrons from the valence band are promoted to the conduction band leaving positive holes in the valence band. The generated electron–hole pair moves to the semiconductor surface and reacts with organic

* Corresponding author. Tel.: +91 22 22844219; fax: +91 22 22816750.
E-mail address: ymalghe@yahoo.com (Y.S. Malghe).
Peer review under responsibility of King Saud University.

Production and hosting by Elsevier

http://dx.doi.org/10.1016/j.jscs.2015.07.001
1319-6103

pollutants degrading them into non hazardous by-products. Titanium dioxide (TiO_2) based photocatalysts have been the most widely studied materials in the field of photocatalysis [7–10]. Besides TiO_2, ZnO has been intensively studied due to its photosensitivity, nontoxic nature, abundant availability, and low cost [11,12]. ZnO has several advantages compared to TiO_2. It absorbs a large portion of the UV spectrum and more light quanta [13,14]. However, ZnO is a wide band gap (3.3 eV) semiconductor, which means it can be activated only in UV light. The solar spectrum consists of 4% UV and 42% visible light. Various strategies have been adopted to extend the spectral response of ZnO to visible light, it includes doping with transition metals, surface modification, semiconductor coupling etc. [15–18]. CdS is a very important II–VI semiconductor with a band gap of 2.42 eV [19]. CdS is considered to be the most suitable visible light sensitizer for ZnO because the lattice structure of CdS is similar to that of ZnO, which could help to build a close interaction between the two semiconductors. Spanhel et al. reported [20] that photoexcited electron transfer efficiency from CdS to ZnO is much less than that from CdS to TiO_2. Also, ZnO/CdS heterostructure is widely used in PN junction solar cells due to its excellent carrier transport at the interface [21]. It is reported that doping of non-metals such as C, N and S into the ZnO lattice creates an intermediate energy level just above the valence band of ZnO and decreases the band gap [22,23]. Among this C doping is reported to be very efficient for visible light induced photocatalysis. C doping promotes the separation of photoelectrons and holes by channelizing the photo excited electrons to nanosized C on the surface of the catalyst, thereby reducing the rate of recombination [24]. Therefore, in the present work we report the synthesis of C/ZnO/CdS nanocomposite. Also, the visible light photocatalytic activity of the synthesized nanocomposite was investigated for degradation of 4-CP. In this work C/ZnO/CdS nanocomposite was synthesized using the microemulsion method. The major advantages of this method are low reaction temperature, short processing time, and control of morphology, the attractive effect of preventing agglomeration in the nanoparticles formed and nanoparticles prepared is homogeneous [25,26].

2. Materials and methods

2.1. Materials

4-Chlorophenol (4-CP) was procured from SD Fine Chemicals, Mumbai and used without any further purification. Cyclohexane, n-butanol, N,N,N-cetyl trimethyl ammonium bromide (CTAB), acetone, cadmium nitrate ($Cd(NO_3)_2{\cdot}4H_2O$), zinc nitrate (($Zn(NO_3)_3{\cdot}6H_2O$), sodium sulfide flakes (Na_2S), sodium hydroxide (NaOH) and ethanol are of AR grade, procured from SD Fine Chemicals, Mumbai and used without further purification.

2.2. Preparation of catalyst

2.2.1. Preparation of C/ZnO/CdS nanocomposite

14.4 mL of zinc nitrate, 2.95 g CTAB, 4 mL n-butanol and 17.6 mL cyclohexane were added in a beaker and solution was stirred for 30 min. To this solution, 14.4 mL of 0.5 M cadmium nitrate was added slowly with constant stirring. In another beaker 14.4 mL of 2 M sodium hydroxide, 2.95 g CTAB, 4 mL n-butanol, 17.6 mL cyclohexane and 14.4 mL 0.5 M sodium sulfide were taken and the mixture was stirred for 30 min. Both the solutions were mixed with each other with constant stirring. The resultant mixture was transferred to a 250 mL Teflon-lined stainless steel autoclave, followed by heating at 150 °C for 1 h. The residue formed was separated by centrifugation, washed with distilled water followed by ethanol and finally with acetone, then dried in an oven at 40 °C. The product thus formed was used as a precursor. The precursor was calcined in air at 300 °C for 2 h to get a C/ZnO/CdS composite. ZnO/CdS nanocomposite was obtained by heating the precursor at 500 °C for 2 h.

2.2.2. Preparation of CdS nanoparticles

In a typical procedure, 50 mL of 1 M Cadmium nitrate, 25 mL distilled water, 25 mL ethanol and 0.34 g CTAB were mixed in a beaker. To this solution 50 mL of 1 M Na_2S, 25 mL ethanol and 25 mL distilled water were added with vigorous stirring. Following this 20 mL of 2 M NaOH was added with vigorous stirring which gives a light yellow precipitate. This mixture was transferred to a 250 mL Teflon-lined stainless steel autoclave, followed by heating at 100 °C for 2 h. Following this, it was cooled to room temperature and the residue obtained was separated by centrifugation, washed several times with distilled water, ethanol and finally with acetone, then dried in oven at 40 °C, to get the final product.

2.2.3. Preparation of pure and C doped ZnO

Pure and C doped ZnO was prepared using the procedure reported in our previous work [22]. 1 M solution of zinc nitrate was prepared by dissolving 29.74 g $Zn(NO_3)_2{\cdot}6H_2O$ in 100 mL distilled water. 2 M sodium hydroxide solution was prepared by dissolving 8 g of NaOH in 100 mL of distilled water. To 28.8 mL of 1 M zinc nitrate, 35.5 mL cyclohexane, 8 mL butanol and 5.90 g CTAB were added. In another solution 28.8 mL of 2 M NaOH, 35.5 mL cyclohexane, 8 mL butanol and 5.90 g CTAB were mixed. Both these solutions were stirred continuously with the help of a magnetic stirrer to form clear solutions. These clear solutions were mixed with each other. The mixture was transferred to a 250 mL Teflon lined autoclave and heated in an oven at 150 °C for 1 h. After 1 h the autoclave was cooled to room temperature. Solid product formed was separated by filtration, washed with distilled water followed by ethanol and finally with acetone and dried in an oven at 60 °C. The precursor thus formed was calcined at different temperatures to yield C doped and pure ZnO.

2.3. Characterization

X-ray diffraction (XRD) patterns of the product obtained in the present work were recorded using an X-ray diffractometer (Rigaku; model Miniflex-II) with monochromatic Cu K-α radiation (λ = 1.54178 Å). Surface morphology, size and shape of the samples were examined using field emission scanning electron microscope (FE-SEM) (JEOL; model JSM-6360A and ZEISS; model Ultra-55) and transmission electron microscope (Philips; model CM200). Optical properties were measured using a Shimadzu UV–vis spectrophotometer

(Shimadzu; model 1800). Photoluminescence spectra of samples were recorded at room temperature using Fluorescence spectrophotometer (Perkin Elmer-LS-55) with an excitation wavelength of 325 nm.

2.4. Photocatalytic activity study

Photocatalytic activities of the nanocomposite synthesized in the present work were evaluated for the degradation of 4-CP. Reaction suspension was prepared by adding 0.05 g of photocatalyst in 100 mL, 10 ppm 4-CP solution. This aqueous suspension was stirred in the dark for 30 min to attain adsorption–desorption equilibrium. Later, the solution was irradiated with visible light. Visible light irradiation was carried out in a photo reactor using a compact fluorescent lamp (65 W, $\lambda > 420$ nm, Philips). Intensity of the light reaching the test solution is 42 W/m^2. Temperature of the test solution was maintained constant throughout the experiment by circulating water around the solution. The amount of 4-CP was monitored by sampling out 5 mL of aliquot solution at regular time intervals. The catalyst was first separated by centrifugation and the concentration of 4-CP in the supernatant solution was estimated using UV–visible spectrum recorded in the wavelength range of 200–800 nm. Concentration of 4-CP in the test solution during the photocatalytic degradation process was also evaluated using the HPLC technique. For this study HPLC (HPLC; 1200, Agilent) equipped with a Zorbax C-18 column (250 mm × 4.6 mm × 5 μm) with a diode array detector was used. Mobile phase used to record the chromatogram is a mixture of water and methanol solution in a ratio of 50:50 (v/v). Injection volume of the sample used and flow rate of mobile phase are 20 μL and 1.0 mLmin^{-1} respectively.

3. Results and discussion

3.1. XRD study

XRD patterns of CdS, C doped ZnO and C/ZnO/CdS nanocomposite are presented in Fig. 1. X-ray diffraction pattern of CdS (Fig. 1a) shows peaks at 2θ equal to 26.89, 44.122 and 52.19° which correspond to (111), (220) and (311) crystal planes of face-centered cubic (fcc) CdS (JCPDS card No. 75-0581). Broadening of these peaks indicates that CdS prepared in this work has small particle size. Fig. 1b shows the XRD pattern of ZnO obtained at 300 °C. Peaks at 31.80, 34.44, 36.28, 47.46, 56.65, 62.86, 66.46, 67.98, 69.04, 72.64 and 77.0° correspond to (100), (002), (101), (102), (110), (103), (200), (112), (201), (004) and (202) crystal planes of ZnO respectively which reveals that the ZnO sample has a hexagonal wurtzite structure (JCPDS card No. 36-1451). Fig. 1c represents XRD pattern of C/ZnO/CdS nanocomposite. This pattern shows the presence of two sets of diffraction peaks corresponding to ZnO as well as the CdS phase indicating the formation of ZnO/CdS composite. No other impurity phases are present. XRD pattern shows that, the (111) peak of CdS shifts from 26.89° to 26.51°, (220) peak shifts from 44.12° to 43.84° and the (311) peak shifts from 52.19° to 51.94°. It also shows that the intensity of ZnO peaks decreases with CdS coupling. Average crystallite size of CdS and ZnO nanoparticles was calculated using Debye–Scherrer equation and is found to be 8 and 26 nm respectively.

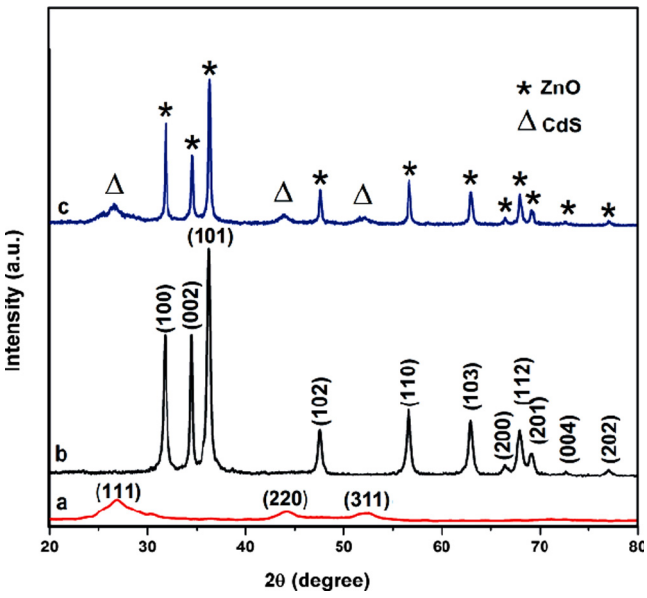

Figure 1 XRD patterns of (a) pure CdS (b) C doped ZnO and (c) C/ZnO/CdS nanocomposite.

3.2. EDX study

Fig. S1 shows EDX spectra recorded for CdS, ZnO, C doped ZnO and C/ZnO/CdS nanocomposite. EDX spectra of C/ZnO/CdS composite (Fig. S1d) reveal the existence of Zn, Cd, C, O and S elements, which indicates the formation of CdS nanoparticles on the surface of C doped ZnO nanorods. Amounts of different elements present in the photocatalyst were estimated from EDX spectra and are presented in Table 1.

3.3. SEM study

FE-SEM images of CdS, C doped ZnO and C/ZnO/CdS nanocomposite are shown in Fig. 2. Fig. 2a shows that the CdS particles are spherical in shape having a particle size which varies between 6 and 10 nm. C doped ZnO prepared

Table 1 Characteristic properties of photocatalysts.

Sample	C content Wt%	O content Wt%	Cd content Wt%	S content Wt%	Zn content Wt%	Band gap (E_g) eV
CdS	–	–	69.19	30.81	–	1.98
Pure ZnO	–	1.82	–	–	98.18	3.04
C doped ZnO	3.87	2.41	–	–	93.72	2.47
C/ZnO/CdS	3.01	2.18	30.54	13.79	50.48	2.20

Chemical composition was obtained from EDX analysis.
Band gap energy was calculated from diffuse reflectance spectra using Kubelka–Munk equation.

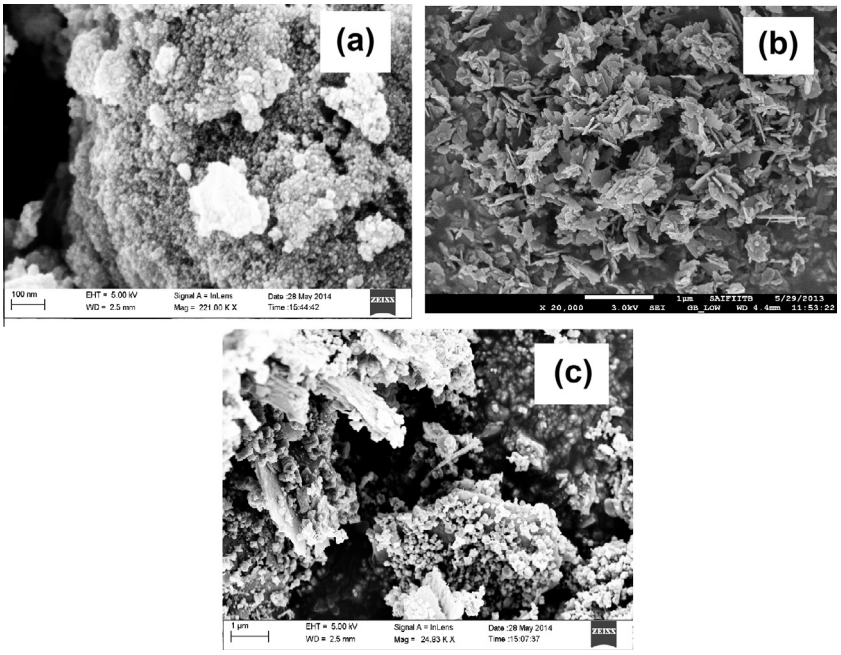

Figure 2 SEM images of (a) pure CdS, (b) C doped ZnO and (c) C/ZnO/CdS nanocomposite.

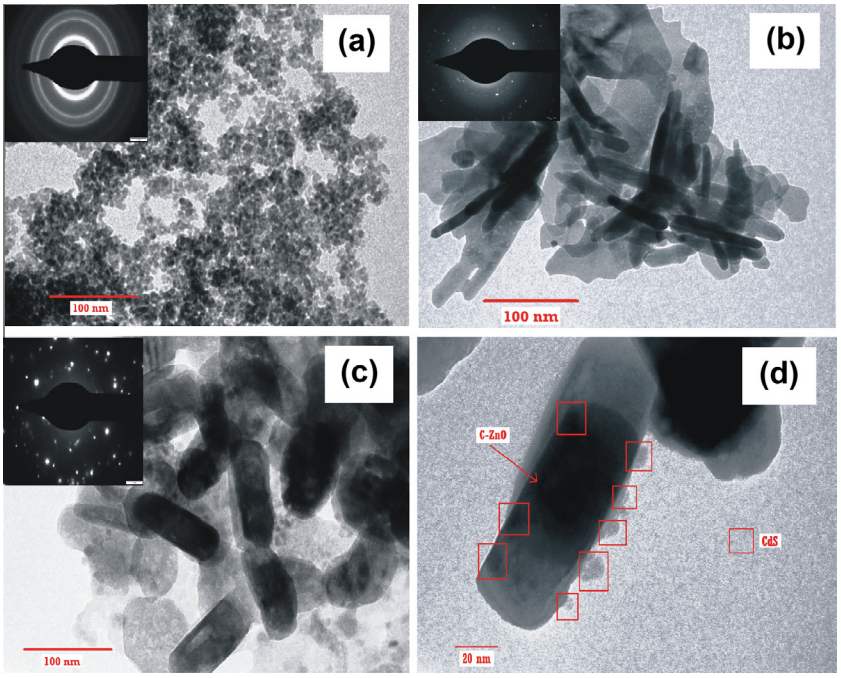

Figure 3 TEM images of (a) pure CdS, (b) C doped ZnO, (c) and (d) C/ZnO/CdS nanocomposite.

at 300 °C is having irregular shape (Fig. 2b). Fig. 2c shows that the C/ZnO/CdS nanocomposite consists of a mixture of flakes (C/ZnO) and spherical particles (CdS).

3.4. TEM study

Fig. 3a represents the TEM image of CdS powder. It indicates that CdS particles are spherical in shape with an average particle size ~9 nm. It also shows that CdS nanoparticles are well dispersed. Fig. 3b indicates that C doped ZnO prepared at 300 °C is having a rod like structure with diameter and length varying between 20 and 30 and 150–400 nm respectively. It shows that ZnO nanorods are encapsulated by an amorphous C layer. Fig. 3c and d represents TEM images of the C/ZnO/CdS nanocomposite. It shows that CdS nanoparticles are successfully deposited on the surface of C doped ZnO nanorods. The length of the C doped ZnO nanorods decreased

to 110 nm and width increased to 40 nm due to the deposition of CdS nanoparticles on its surface. Inset selected electron diffraction (SAED) patterns show the crystalline nature of the samples.

3.5. UV–visible absorption study

Fig. S2 illustrates the UV–visible absorption spectra of pure ZnO, CdS, C doped ZnO and C/ZnO/CdS. Pure ZnO obtained at 500 °C is a white colored powder having an absorption cut-off edge at 402 nm, corresponding to a band gap of 3.08 eV. Black gray color C doped ZnO sample obtained after heating the ZnO precursor at 300 °C gives an absorption edge at 460 nm, having a band gap of 2.69 nm. This shows that C-doped ZnO exhibits a red shift and extends the absorption edge from UV to visible region. This figure shows that pale yellow colored CdS nano powder exhibits a band edge at 540 nm (2.29 eV), which is consistent with the band gap of the cubic CdS phase. Band edge for C/ZnO/CdS is observed at 508 nm (2.42 eV), which indicates the ability of these nanocomposites to harvest visible light from solar radiation. These results show that CdS loading effectively increases the photoabsorption capacity of C doped ZnO nanorods in the visible region.

3.6. Diffuse reflectance spectroscopic study

Diffuse reflectance spectra of pure ZnO, CdS, C doped ZnO and C/ZnO/CdS were recorded and are presented in Fig. 4. From these spectra optical band-gap energy (E_g) was calculated using Kubelka–Munk equation

$$F(R_\infty) = \frac{(1 - R_\infty)^2}{2R_\infty} \quad (1)$$

where, R_∞ is the diffuse reflectance of the examined samples $R_\infty = R_{sample}/R_{standard}$ and $F(R_\infty)$ is called the remission or Kubelka–Munk function [27]. The band gap is obtained using the equation:

$$(F(R_\infty) \cdot hv)^2 = A(hv - E_g) \quad (2)$$

The variation of $(F(R_\infty)\cdot hv)^2$ versus hv was plotted and the straight line range of these plots is extended on the x-axis (hv) to obtain the values of optical band gap (E_g). Band gap energies of all the samples were estimated using the plot of $(F(R_\infty)\cdot hv)^2$ versus photon energy (hv) (Kubelka–Munk equation) and are presented in Table 1. Band gap energies of pure and C doped ZnO, pure CdS and C/ZnO/CdS are 3.08, 2.47, 1.98 and 2.20 eV, respectively.

3.7. Photoluminescence (PL) study

Room temperature PL spectra of pure ZnO, CdS, ZnO/CdS, C doped ZnO and C/ZnO/CdS nanocomposite were recorded and are shown in Fig. 5. Pure ZnO exhibits emission bands at 405, 430, 460, and 485 nm and the observed spectrum is in good agreement with PL results of ZnO reported in the literature [28,29]. Emission centered at 405 nm is attributed to excitonic recombination corresponding to the near band edge emission of ZnO [30]. The emission in the blue region at about 430 nm is associated with the electronic transition between the excitonic level and interstitial oxygen (Oi). The emission in the blue-green region at 460 nm is attributed to the electron transition between a shallow donor (Zni) and a deep acceptor. The emission band in the green region (485 nm) is attributed to stoichiometry related defects and these are generally attributed to zinc vacancies as well as interstitial zinc and structural defects [28,31]. Pure CdS shows a broad emission band between 500 and 620 nm which is ascribed to surface defects associated with the cadmium and sulfur vacancies [32]. PL spectra of the ZnO/CdS nanocomposite show luminescence at 535 nm. The emission bands in the ZnO/CdS heteronano-structures are attributed to the various transitions: (i) from conduction band to deep acceptor levels (Oi or OZn), (ii) from deep donor levels (VOZni) to the valence band, and (iii) from shallow donor levels (Zni) to shallow acceptor levels (VZn and Oi) [33]. The emission intensity related to defect states in the visible region in the ZnO/CdS composite is relatively lower compared to that in pure ZnO. In the ZnO/CdS nanocomposite, CdS nanoparticles act as a sulfur dopant, which reduces the defect emission from the surface of ZnO nanorods [27]. In the case of ZnO/CdS heteronanostructures, the emission maximum

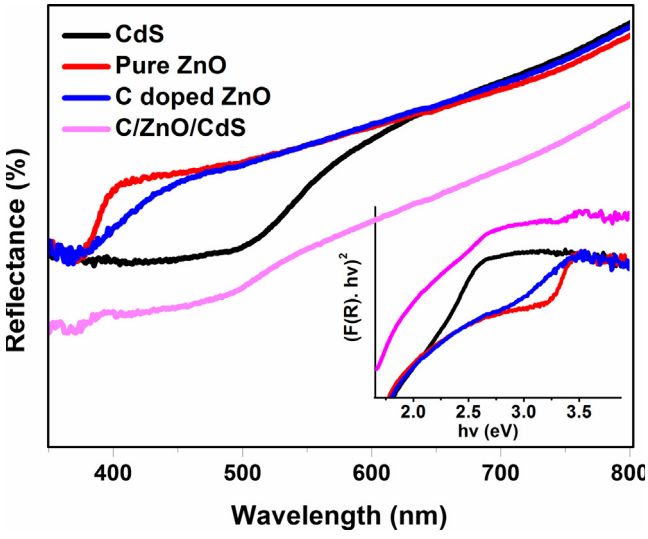

Figure 4 Diffuse reflectance spectra of CdS, pure ZnO, C doped ZnO and C/ZnO/CdS nanocomposite. The inset shows plot of $(F(R)\cdot hv)^2$ versus hv (using Kubelka–Munk method).

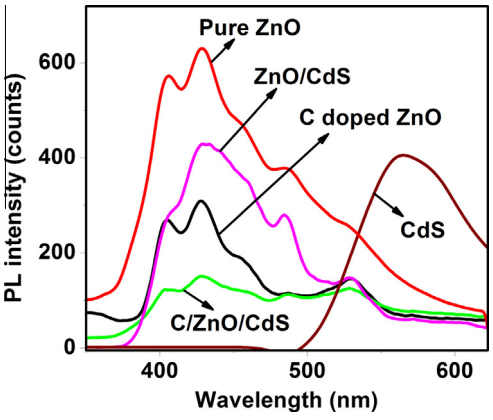

Figure 5 Photoluminescence spectra of pure ZnO, CdS, ZnO/CdS, C doped ZnO and C/ZnO/CdS heteronanostructures.

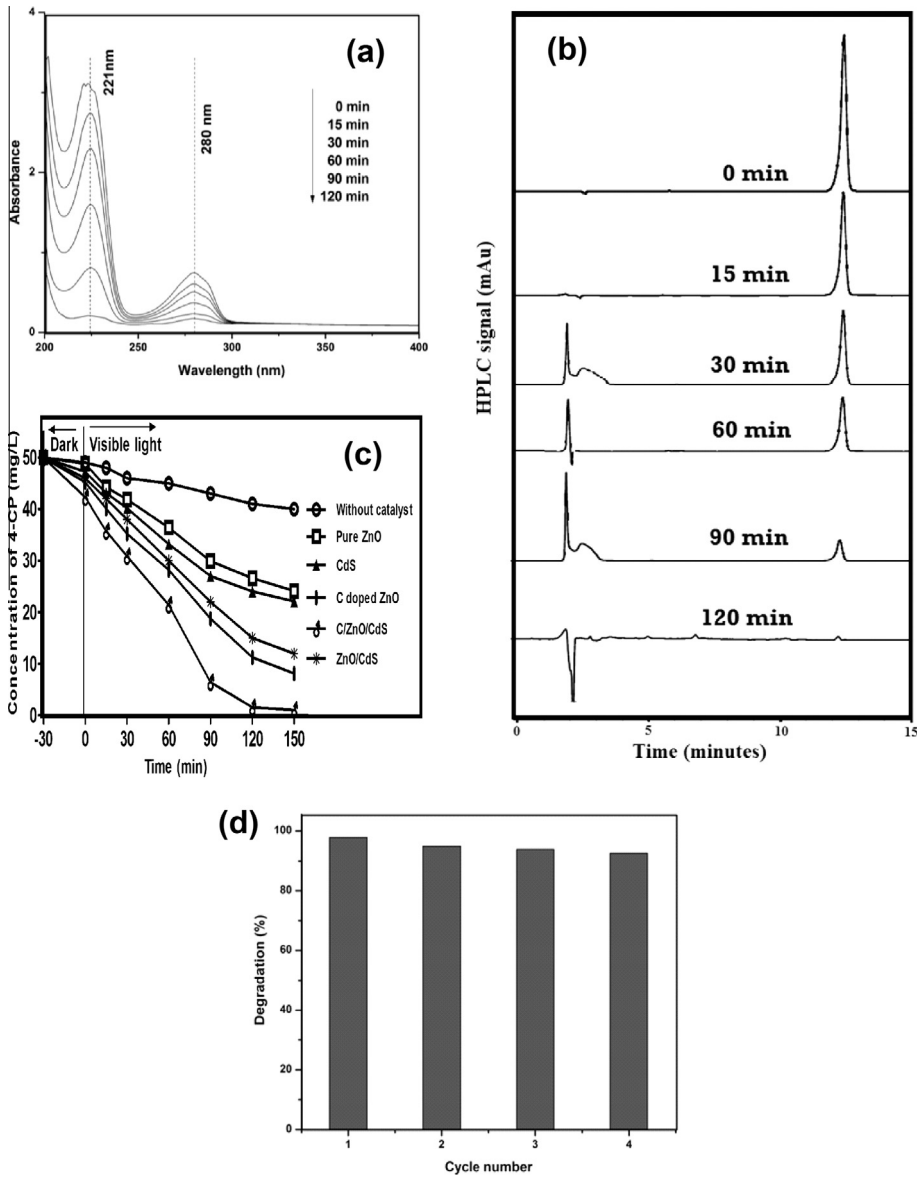

Figure 6 (a) UV–visible spectra of 4-CP solution irradiated with visible light at different time intervals in the presence of the C/ZnO/CdS nanocomposite, (b) HPLC chromatograms of 4-CP solution irradiated with visible light at different time intervals in the presence of the C/ZnO/CdS photocatalyst, (c) visible light photocatalytic degradation of 4-CP in the presence of different catalysts and (d) reuse of the photocatalyst.

(530 nm) is blue, shifted by about 36 nm compared to pure CdS nanoparticles (566 nm). This is the evidence for electron transfer from CdS to ZnO on excitation. It is observed from Fig. 5 that PL intensity of C doped ZnO is much lower as compared to that of pure ZnO. It can be seen that the C/ZnO/CdS nanocomposite gives lower intensity PL peak as compared to ZnO, C doped ZnO and ZnO/CdS composite, which is attributed to its higher photocatalytic activity. This is because, lower the excitonic PL intensity, stronger the capacity of dopants to capture photo-induced electrons, higher the separation rate of photoinduced electrons and holes, and higher the photocatalytic activity. Photoluminescence effect, is present as the result of direct radiative recombination, lower recombination of generated carriers causes the decrease of light emission intensity. However, this process simultaneously increases the photocatalytic activity of the semiconductors [34,35].

3.8. Photocatalytic activity study

Visible light photocatalytic degradation of 4-CP was studied in the presence of nanosized pure ZnO, CdS, C doped ZnO and C/ZnO/CdS photocatalyst. Representative UV visible spectra of aqueous solution of 4-CP irradiated with visible light at different time intervals in the presence of C/ZnO/CdS nanocomposite (prepared at 300 °C) were recorded and are presented in

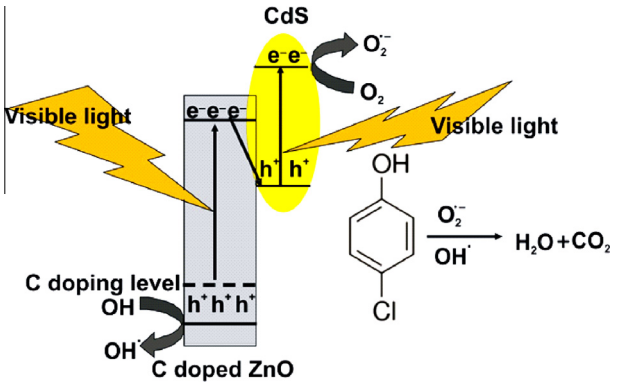

Figure 7 Proposed Z-scheme mechanism for the degradation of 4-CP in the presence of C/ZnO/CdS nanocomposite.

Fig. 6a. These spectra show two peaks located at 221 and 280 nm. As irradiation time increased the peak maxima at both these wavelengths decreases due to the photocatalytic degradation of 4-CP. The study indicates ~98% TCP is degraded in 120 min.

The amount of 4-CP in the test solution during the photocatalytic degradation process was also evaluated using the HPLC technique. HPLC chromatograms of test solution irradiated at different time intervals in the presence of C/ZnO/CdS nanocomposite were recorded and are presented in Fig. 6b. The chromatogram of the standard solution gives a peak at retention time of 12.74 min, which is characteristic of 4-CP. As irradiation time increased the intensity of the peak at 12.74 min decreases, indicating degradation of 4-CP and ~98% mineralization occurred in 120 min. It is known that 4-CP degradation leads to the formation of a mixture of byproducts such as benzoquinone and hydroquinone which further reacts with hydroxyl radicals and forms CO_2 and H_2O.

Fig. 6c shows the photocatalytic activity of pure ZnO, CdS, C doped ZnO, C/ZnO/CdS and ZnO/CdS nanocomposite for the degradation of 4-CP solution under visible light irradiation. It shows that C/ZnO/CdS nanocomposite exhibits better photocatalytic activity as compared to other photocatalysts. The enhanced photocatalytic activity is due to effective CdS loading on C doped ZnO nanorods and increase in photoabsorption capacity in the visible region.

C/ZnO/CdS nanocomposite prepared at 300 °C exhibits better photocatalytic activity therefore its stability was studied. Stability tests were performed by repeating the reaction four times using the recovered photocatalyst and the data obtained are presented in Fig. 6d. This figure reveals that there is no noticeable decrease in photocatalytic activity up to the fourth cycle. It indicates that C/ZnO/CdS nanocomposite prepared in the present work is a highly stable and reusable photocatalyst.

3.9. Degradation mechanism

Photocatalysis is a process in which the reaction occurs when the semiconductor interacts with light of sufficient energy to produce reactive oxidizing species (ROS), which in turn give rise to photocatalytic transformation of organic pollutants. In this process reactive oxidizing species were produced via two simultaneous reactions. In the first, photogenerated holes oxidize dissociative adsorbed H_2O and in second reduction of the electron acceptor takes place by photoexcited electrons. Typically, the reactive photogenerated holes react with adsorbed OH^- on the catalyst surface to form hydroxyl ($OH^{\cdot}$) radicals and in the second reaction the excited electrons in the conduction band move to the surface and further transfer to surface-adsorbed oxygen producing superoxide anion radicals ($O_2^{\cdot-}$), which then react with H_2O to produce $OH^{\cdot}$ radicals which are known to be the most powerful oxidizing species [23,24]. These two simultaneous reactions produce hydroxyl and superoxide radical anions respectively. 4-CP decomposes by reaction with $OH^{\cdot}$ and $O_2^{\cdot-}$ reactive ions. The possible Z-scheme mechanism [36] is presented in Fig. 7. C doping can effectively decrease the band gap of ZnO by forming the energy level just above the valence band of ZnO and also creates oxygen vacancies. If a system is irradiated with visible light, photoexcited electrons in the higher conduction band minimum (CBM) of CdS transfers to the lower CBM of ZnO. This results in lowering of reduction power of transferred electrons. Some of the photoexcited electrons in the ZnO semiconductor with a lower CBM could combine with holes in the higher VBM of CdS. More powerful excited electrons and holes can be retained on both counterparts, which are responsible for the formation of highly reactive superoxide radical anion ($O_2^{\cdot-}$) and hydroxyl radicals ($OH^{\cdot}$). These highly oxidative species effectively decompose the organic substrate into H_2O and CO_2. C/ZnO/CdS heterostructure coupling on photocatalytic degradation of 4-CP by Z-scheme, shows a threefold increase in photocatalytic activity, due to charge separation and efficient interfacial charge transfer [17].

4. Conclusions

In summary, we have prepared the C/ZnO/CdS nanocomposite using the microemulsion method. XRD patterns of the composite confirmed the presence of cubic CdS and wurtzite ZnO phases. Band gap study reveals that C/ZnO/CdS coupling shows enhanced visible light photo absorption capacity i.e. red shift in the visible region. PL study shows quenching of PL intensity and the synergistic interaction between C doped ZnO and CdS in the C/ZnO/CdS heteronanostructures. C/ZnO/CdS nanocomposite exhibits better visible light photocatalytic activity for degradation of 4-CP as compared to bare as well as C doped ZnO. The higher photocatalytic activity of C/ZnO/CdS nanocomposite is attributed to the efficient charge separation and also the synergistic interaction between C/ZnO and CdS. C/ZnO/CdS nanocomposite prepared in the present work is a highly stable and reusable photocatalyst.

Acknowledgments

Authors are thankful to Sophisticated Analytical Instrumentation Facility (SAIF), IIT, Mumbai for availing the SEM and TEM facilities. One of the authors Atul B. Lavand is grateful to University Grants Commission (UGC), New Delhi for providing research fellowship.

Appendix A. Supplementary data

Supplementary data associated with this article can be found, in the online version, at http://dx.doi.org/10.1016/j.jscs.2015.07.001.

References

[1] G. Waldner, M. Pourmodjib, R. Baauer, M. Neumann-spallart, Photoelectrocatalytic degradation of 4-chlorophenol and oxalic acid on titanium dioxide electrodes, Chemosphere 50 (2003) 989–998.

[2] M.L. Hitchman, F. Tian, Studies of TiO_2 thin films prepared by chemical vapour deposition for photocatalytic and photoelectrocatalytic degradation of 4-chlorophenol, J. Electroanal. Chem. 538–539 (2002) 165–172.

[3] S. Ahmed, M.G. Rasul, R. Brown, M.A. Hashib, Influence of parameters on the heterogeneous photocatalytic degradation of pesticides and phenolic contaminants in wastewater: a short review, J. Environ. Manag. 92 (2011) 311–330.

[4] V. Vo, T.P.T. Thi, H.Y. Kim, S.J. Kim, Facile post synthesis and photocatalytic activity of N-doped ZnO-SBA-15, J. Phys. Chem. Solids 75 (2014) 403–409.

[5] R. Saravanan, M.M. Khan, V.K. Gupta, E. Mosquera, F. Gracia, V. Narayanan, A. Stephen, $ZnO/Ag/Mn_2O_3$ nanocomposite for visible light induced industrial textile effluent degradation, uric acid and ascorbic acid sensing and antimicrobial activity, RSC Adv. 5 (2015) 34645–34651.

[6] M.M. Khan, S.A. Ansari, M.E. Khan, M.O. Ansari, B.K. Min, M.H. Cho, Visible light-induced enhanced photoelectrochemical and photocatalytic studies of gold decorated SnO_2 nanostructures, New J. Chem. 39 (2015) 2758–2766.

[7] S.K. Yadav, S.R. Madeshwaran, J.W. Cho, Synthesis of a hybrid assembly composed of titanium dioxide nanoparticles and thin multi-walled carbon nanotubes using "click chemistry", J. Coll. Int. Sci. 358 (2011) 471–476.

[8] Y. Park, W. Kim, H. Park, T. Tachikawa, T. Majima, W. Choi, Carbon-doped TiO_2 photocatalyst synthesized without using an external carbon precursor and the visible light activity, Appl. Catal. B Environ. 91 (2009) 355–361.

[9] X. Hu, H. Ji, L. Wu, Singlet oxygen photogeneration and 2,4,6-TCP photodegradation at Pt/TiO_2 under visible light illumination, RSC Adv. 2 (2012) 12378–12383.

[10] T.K. Ghorai, Photocatalytic degradation of 4-chlorophenol by $CuMoO_4$-doped TiO_2 nanoparticles synthesized by chemical route, Open J. Phys. Chem. 1 (2011) 28–36.

[11] O. Haibo, H.J. Feng, L. Cuiyan, C. Liyun, F. Jie, Synthesis of carbon doped ZnO with a porous structure and its solar-light photocatalytic properties, Mater. Lett. 111 (2013) 217–220.

[12] S.J. Peatson, D.P. Norton, K. Ip, Y.W. Heo, T. Steiner, Recent progress in processing and properties of ZnO, Prog. Mater. Sci. 50 (2005) 293–340.

[13] C.A.K. Gouvea, F. Wypych, S.G. Moraes, N. Duran, N. Nagata, P. Peralta-Zamora, Semiconductor-assisted photocatalytic degradation of reactive dyes in aqueous solution, Chemosphere 40 (2000) 433–440.

[14] B. Dindar, S. Icli, Unusual photoreactivity of zinc oxide irradiated by concentrated sunlight, J. Photochem. Photobiol. A Chem. 140 (2001) 263–268.

[15] K. Kumar, M. Chitkara, I.S. Sandhu, D. Mehta, S. Kumar, Photocatalytic, optical and magnetic properties of Fe-doped ZnO nanoparticles prepared by chemical route, J. Alloys Comp. 588 (2014) 681–689.

[16] C. Li, T. Ahmed, M. Ma, T. Edvinsson, J. Zhu, A facile approach to ZnO/CdS nanoarrays and their photocatalytic and photoelectrochemical properties, Appl. Catal. B Environ. 138 (2013) 175–183.

[17] F. Xu, Y. Yuan, H. Han, D. Wu, Z. Gao, K. Jiang, Synthesis of ZnO/CdS hierarchical heterostructure with enhanced photocatalytic efficiency under nature sunlight, Cryst. Eng. Comm. 14 (2012) 3615–3622.

[18] R. Saravanan, M. Mansoob Khan, V.K. Gupta, E. Mosquera, F. Gracia, V. Narayanan, A. Stephen, ZnO/AG/CdO nanocomposite for visible light induced photocatalytic degradation of industrial textile influents, J. Coll. Inter. Sci. 452 (2015) 126–133.

[19] S.L. Xiong, B.J. Xi, Y.T. Qian, CdS hierarchical nanostructures with tunable morphologies: preparation and photocatalytic properties, J. Phys. Chem. C 114 (2010) 14029–14035.

[20] L. Spanhel, H. Weller, A. Henglein, Photochemistry of semiconductor colloids. 22. Electron ejection from illuminated cadmium sulfide into attached titanium and zinc oxide particles, J. Am. Chem. Soc. 109 (1987) 6632–6635.

[21] L. Stolt, J. Hedstrom, J. Kessler, M. Ruckh, K.O. Velthaus, H.W. Schock, $ZnO/CdS/CuInSe_2$ thin-film solar cells with improved performance, Appl. Phys. Lett. 62 (1993) 597–599.

[22] A.B. Lavand, Y.S. Malghe, Synthesis characterization, and visible light photocatalytic activity of nanosized carbon doped zinc oxide, Int. J. Photochem. 790153 (2015) 1–9.

[23] A. Mills, S.L. Hunte, An overview of semiconductor photocatalysis, J. Photochem. Photobiol. A 108 (1997) 1–35.

[24] M. Pelaez et al, A review on the visible light active titanium dioxide photocatalysts for environmental applications, Appl. Catal. B Environ. 125 (2012) 331–349.

[25] M. Inoguchi, K. Suzuki, K. Kageyama, H. Takagi, Y. Sakabe, Monodispersed and well-crystallized zinc oxide nanoparticles fabricated by microemulsion method, J. Am. Ceram. Soc. 91 (2008) 3850–3855.

[26] A.B. Lavand, Y.S. Malghe, Nano sized C doped TiO_2 as a visible light photocatalyst for the degradation of 2,4,6-trichlorophenol, Adv. Mater. Lett. (2015), http://dx.doi.org/10.5185/amlett.2015.5800.

[27] M. Misra, P. Kapur, C. Ghanshyam, M.L. Singla, ZnO@CdS core-shell thin film: fabrication and enhancement of exciton life time by CdS nanoparticle, J. Mater. Sci. 24 (2013) 3800–3804.

[28] X. Chong, L. Li, X. Yan, D. Hu, H. Li, Y. Wang, Synthesis, characterization and room temperature photoluminescence properties of Al doped ZnO nanorods, Physica E 44 (2012) 1399–1405.

[29] K. Zhong, J. Xia, H.H. Li, C.L. Liang, P. Liu, Y.X. Tong, Morphology evolution of one-dimensional-based ZnO nanostructures synthesized via electrochemical corrosion, J. Phys. Chem. C 113 (2009) 15514–15523.

[30] F. Xu, V. Volkov, Y. Zhu, H. Bai, A. Rea, N.V. Valappil, W. Su, X. Gao, I.L. Kuskovsky, H. Matsui, Long electron–hole separation of ZnO–CdS core–shell quantum dots, J. Phys. Chem. C 113 (2009) 19419–19423.

[31] Y.L. Wu, A.I.Y. Tok, F.Y.C. Boey, X.T. Zeng, X.H. Zhang, Surface modification of ZnO nanocrystals, Appl. Surf. Sci. 253 (2007) 5473–5479.

[32] Q. Xiao, C. Xiao, Surface-defect-states photoluminescence in CdS nanocrystals prepared by one-step aqueous synthesis method, Appl. Surf. Sci. 255 (2009) 7111–7114.

[33] S. Khanchandani, S. Kundu, A. Patra, A.K. Ganguli, Shell thickness dependent photocatalytic properties of ZnO/CdS core-shell nanorods, J. Phys. Chem. C 116 (2012) 23653–23662.

[34] J.G. Yu, H.G. Yu, B. Chen, X.J. Zhao, J.C. Yu, W.K. Ho, The effect of calcination temperature on the surface microstructure and photocatalytic activity of TiO_2 thin films prepared by liquid phase deposition, J. Phys. Chem. B 107 (2003) 13871–13879.

[35] D. Wojcieszak, D. Kaczmarek, J. Domaradzki, M. Mazur, Correlation of photocatalysis and photoluminescence effect in relation to the surface properties of TiO_2: Tb thin films, Int. J. Photoenergy 526140 (2013) 1–9.

[36] X. Wang, G. Liu, Z.G. Chen, F. Li, L. Wang, G. Lu, H.M. Cheng, Enhanced photocatalytic hydrogen evolution by prolonging the lifetime of carriers in ZnO/CdS heterostructures, Chem. Comm. 23 (2009) 3452–3454.